THE JOURNAL OF BIOLOGICAL CHEMISTRY VOL. 287, NO. 31, pp. 26038–26051, July 27, 2012

Biological Significance of Nuclear Localization of Mitogen-activated Protein Kinase Pmk1 in Fission Yeast*

Received for publication, January 24, 2012, and in revised form, May 30, 2012 Published, JBC Papers in Press, June 8, 2012, DOI 10.1074/jbc.M112.345611

Laura Sánchez-Mir[‡1,2], Alejandro Franco[‡1], Marisa Madrid[‡], Jero Vicente-Soler[‡], M. Antonia Villar-Tajadura[§], Teresa Soto[‡], Pilar Pérez[§], Mariano Gacto[‡], and José Cansado[‡3]

From the [‡]Yeast Physiology Group, Department of Genetics and Microbiology, Facultad de Biología. Universidad de Murcia, 30071 Murcia, Spain and the [§]Instituto de Biología Funcional y Genómica, Consejo Superior de Investigaciones Científicas/Departamento de Microbiología y Genética, Universidad de Salamanca, 37007 Salamanca, Spain

Background: Nuclear translocation is crucial for proper functioning of MAPKs.
Results: Although most of MAPK Pmk1-driven functions are carried out independently of its presence into the nucleus, localization at this compartment allows down-regulation by phosphatases.
Conclusion: Constitutive nuclear localization of Pmk1 is important to modulate its overall biological activity.
Significance: These results highlight the relevance of the spatial control of MAPK activity.

Mitogen-activated protein kinase (MAPK) signaling pathways play a fundamental role in the response of eukaryotic cells to environmental changes. Also, much evidence shows that the stimulus-dependent nuclear targeting of this class of regulatory kinases is crucial for adequate regulation of distinct cellular events. In the fission yeast *Schizosaccharomyces pombe*, the cell integrity MAPK pathway, whose central element is the MAPK Pmk1, regulates multiple processes such as cell wall integrity, vacuole fusion, cytokinesis, and ionic homeostasis. In non-stressed cells Pmk1 is constitutively localized in both cytoplasm and nucleus, and its localization pattern appears unaffected by its activation status or in response to stress, thus questioning the biological significance of the presence of this MAPK into the nucleus. We have addressed this issue by characterizing mutants expressing Pmk1 versions excluded from the cell nucleus and anchored to the plasma membrane in different genetic backgrounds. Although nuclear Pmk1 partially regulates cell wall integrity at a transcriptional level, membrane-tethered Pmk1 performs many of the biological functions assigned to wild type MAPK like regulation of chloride homeostasis, vacuole fusion, and cellular separation. However, we found that down-regulation of nuclear Pmk1 by MAPK phosphatases induced by the stress activated protein kinase pathway is important for the fine modulation of extranuclear Pmk1 activity. These results highlight the importance of the control of MAPK activity at subcellular level.

Signal transduction pathways include interconnected molecular networks to process and transmit information about the external surroundings. Evidence has been accumulated about the key role of mitogen-activated protein kinase (MAPK) signaling pathways in the response of eukaryotic cells to stress conditions (1). The canonical MAPK module comprises three basic components, MAPK kinase kinase (MAPKKK), MAPK kinase, and MAPK, which are regulated by a sequential cascade of phosphorylation events. Once MAPKs are phosphorylated by a MAPK kinase at threonine and tyrosine residues in the sequence T-X-Y (X = glutamic acid or glycine) within the activation loop, MAPKs directly phosphorylate a wide variety of cytoplasmic substrates or may shift into the nucleus to activate specific transcription factors involved in the transcriptional program required to respond to the environmental stimuli as well as cell cycle regulatory proteins (2). The rod-shaped, fission yeast *Schizosaccharomyces pombe* has emerged as an excellent model organism to study mechanisms and cellular events linked to MAPK activation. This yeast only has three MAPK pathways: the pheromone signaling pathway (3), the stress-activated protein kinase pathway (SAPK), which is homologous to JNK and p38 pathways in mammals (4), and the cell integrity MAPK pathway, homologous to the ERK1/2 pathway (5, 6). This last pathway, whose central element is the MAPK Pmk1 (also known as Spm1), is essential to regulate important processes in *S. pombe* such as cell wall construction and maintenance during stressing conditions, vacuole fusion, cytokinesis, morphogenesis, and ionic homeostasis (5–9).

The cell integrity MAPK module includes Mkh1 (MAPK kinase kinase) and Pek1/Skh1 (MAPK kinase) forming a ternary complex *in vivo*, and the absence of any of these components induces distinct phenotypes involving defects in cytokinesis and vacuole fusion, hypersensitivity to potassium ions, and increased lysis by β-glucanase treatment (5, 6, 9, 10). Pmk1 is activated by phosphorylation in a Pek1-dependent manner at threonine 186 and tyrosine 188 (8, 10) when *S. pombe* cells face adverse conditions like hyper- and hypo-osmotic stress, glucose withdrawal, cell wall damage, and oxidative stress induced by hydroperoxides or pro-oxidants (10). The strong sensitivity to the above stresses displayed by *S. pombe* mutants lacking Pmk1 indicates that the MAPK function is required for cell adaptation and survival under such conditions. The phosphor-

* This work was supported in part by Ministerio de Educación, Cultura y Deporte Grants BFU2011-22517 (to J. C.) and BFU2010-15641 (to P. P.) and 15280/PI/10 from Fundación Séneca, Spain.
[1] Both authors contributed equally to this work.
[2] A predoctoral fellow from Ministerio de Ciencia e Innovación (Formación de Personal Investigador).
[3] To whom correspondence should be addressed: Dept. of Genetics and Microbiology, Universidad de Murcia, Campus Universitario de Espinardo, 30071 Murcia, Spain. E-mail: jcansado@um.es.

ylation of Pmk1 also oscillates along the cell cycle and peaks during cytokinesis, suggesting the existence of a specific signal that activates the cell integrity pathway and regulates septum formation and dissolution (11).

Among the few known cytoplasmic targets for Pmk1 *in vivo* are RNA-binding proteins Rnc1 and Nrd1 (12, 13), whereas nuclear transcription factor Atf1, which is also the main target for Sty1, has been reported to be phosphorylated by Pmk1 under cell wall damage (14). The major negative regulator of Pmk1 activity in growing cells of *S. pombe* is dual specificity phosphatase Pmp1 (15). However, it has been additionally shown that tyrosine phosphatases Pyp1 and Pyp2 and serine/threonine phosphatases Ptc1 and Ptc3, whose transcriptional induction is dependent on the SAPK pathway via Sty1-Atf1, are also able to associate *in vivo* and dephosphorylate activated Pmk1 (11). Although Pmp1, Pyp1, and Ptc1 control the Pmk1 basal activity level, phosphatases Pyp1, Pyp2, and Ptc1 limit Pmk1 hyperactivation during adaptation to osmostress (11).

Nuclear translocation appears crucial for the proper stimulus-dependent functioning of MAPKs in the regulation of distinct cellular processes (2). Mkh1 and Pek1 are cytoplasmic proteins that also locate at the septum area, and Pmk1 is constitutively localized in both cytoplasm and nucleus as well as in the mitotic spindle and septum during cytokinesis (10). It is important to highlight that Pmk1 nucleo/cytoplasmic shuffling appears unaffected by its phosphorylation status in response to environmental stimuli (10), in contrast to the proposed model for ERK1/2 in mammals, where stress or inducing stimuli trigger MAPK transport to the nucleus. These observations suggest that both active and inactive forms of the Pmk1 kinase cross the nuclear membrane, thus raising questions about the biological relevance of its nuclear localization. In this work we have addressed this issue by obtaining a fission yeast mutant expressing a Pmk1 version excluded from the cell nucleus and located to the plasma membrane. Such a system provides an ideal tool to study the biological significance of nuclear exclusion of a MAPK. Complete characterization of this mutant has revealed the existence of an exquisite regulatory mechanism controlling proper spatial/temporal activity of this important class of regulatory kinases.

EXPERIMENTAL PROCEDURES

Strains and Growth Conditions—The *S. pombe* strains (listed in Table 1) were grown with shaking at 28 °C in YES[4] or Edinburgh Minimal Media (United States Biological) medium with 2% of glucose (16) and supplemented with adenine, leucine, histidine, or uracil (100 mg/liter, Sigma). Mutant strains were obtained by standard transformation procedures or by mating followed by random spore analysis (17). Transformation of yeast strains was performed by the lithium acetate method as described elsewhere (17). In experiments performed with *cdc25-22*-thermosensitive mutant strains, the cells were grown in YES medium to an $A_{600} = 0.2$ at 25 °C (permissive temperature), shifted to 37 °C for 3.5 h, and released from the growth arrest by transfer back to 25 °C. *Escherichia coli* DH5αF′ was employed as host to propagate plasmids by growth at 37 °C in Luria-Bertani medium plus 50 μg/ml ampicillin.

Gene Disruption—The *rho2*$^+$, *pck2*$^+$, *atf1*$^+$, and *mbx1*$^+$ null mutants were obtained by entire deletion of the corresponding coding sequences and their replacement with the KanMX6 cassette by PCR-mediated strategy using plasmid pFA6a-kanMX6 as template (18).

Gene Fusion and Site-directed Mutagenesis—Integrative plasmid pIL-pmk1:GFP contains regulatory sequences plus *pmk1*$^+$ ORF fused at its 3′ end to the green fluorescent protein (GFP) (10). To construct plasmid pIL-pmk1:GFP:C*AAX*, *pmk1*$^+$ ORF plus regulatory sequences were amplified by PCR using pIL-pmk1:GFP as template employing the 5′-oligonucleotide PMKGF-5 (CCTTATCTAGATTTCTCATTGCCGCTTCTG, which hybridizes at positions 313–330 upstream of the *pmk1*$^+$ ATG start codon and contains a XbaI site) and the 3′-oligonucleotide GFPC*AAX*-3 (CCTTACCCGGGTTATGAAATGATGCAGCATTTTGTAGAACTTTTGTATAGTTCATCCATGCC), which hybridizes at the 3′ end of *gfp*$^+$ ORF and incorporates a 27-nucleotide sequence (underlined) encoding the 9 terminal amino acids of Rho2 GTPase that includes a farnesylated cysteine residue (sequence SSTKCCIIS) (19) and followed by a SmaI site. The resulting PCR fragment was digested with XbaI and SmaI and cloned into the integrative plasmid pIL-GFP. Integrative plasmid pIL-pmk1:GFP:RitC was constructed by the overlap extension method with the use of PCR. First, *pmk1*$^+$ ORF plus regulatory sequences was amplified by PCR using pIL-pmk1:GFP as the template employing the 5′-oligonucleotide PMKGF-5 and the 3′-oligonucleotide GFPRit-3 (AAAAAAGGGACAGCTTTTGTATAGTTCATC), which hybridizes at the 3′ end of *gfp*$^+$ ORF and incorporates a 15-nucleotide sequence (underlined) corresponding to the 5 initial amino acids of the C-terminal membrane binding domain of non-C*AAX* GTPase Rit1. Then, a 192-bp DNA fragment encoding the C-terminal membrane binding domain from Rit1 (63-amino acid length) was amplified with the 5′ oligonucleotide GFPRit-5 (GATGAACTATACAAAAGCTGTCCCTTTTTT; complementary to GFPRit-3) and the 3′ oligonucleotide RitS-3 (TCTTACCCGGGTTAAGTTACTGAATCTTTC), which hybridizes at the 3′ end of Rit ORF and is followed by a SmaI site, and employing a human Rit1 cDNA plasmid construct (IMAGE ID 125864, obtained from Source BioScience) as template. The two PCR products were purified by agarose gel electrophoresis, mixed, and subjected to PCR with external primers PMKGF-5 and RitS-3. The final PCR product was then purified, digested with XbaI and SmaI, and cloned into pIL-GFP to obtain pIL-pmk1:GFP:RitC.

To construct plasmid pIL-pmk1:NLS:GFP, *pmk1*$^+$ ORF plus regulatory sequences was amplified by PCR employing the 5′-oligonucleotide PMKGF-5 and the 3′-oligonucleotide SV40LOC-3 (CCTTAGGATCCACTTTGCGTTTTTTTTTAGGGTTATGGCGATTATCATCAG), which hybridizes at the 3′ end of *pmk1*$^+$ ORF and incorporates a 21-nucleotide sequence (underlined) encoding the nuclear localization signal (NLS, sequence PKKKRKV) of the SV-40 virus placed immediately upstream of the TAA stop codon and followed by a BamHI site. PCR amplification generated a DNA fragment that was cleaved with XbaI and BamHI and cloned into

[4] The abbreviations used are: YES, yeast extract plus supplement; NLS, nuclear localization signal; CDCFDA, carboxydichlorofluorescein diacetate.

TABLE 1

***S. pombe* strains used in this study**

All strains are *ade- leu1-32 ura4D-18*.

Strain		Genotype		Source/reference
MM1	h$^+$			Madrid *et al.* 20
MM2	h$^-$			Madrid *et al.* 20
MI102	h$^+$	*pmk1::KanR*		Madrid *et al.* 11
TP319-13c	h$^-$	*pmk1::ura4*$^+$		T. Toda
TK107	h$^-$	*sty1:: ura4*$^+$		Laboratory collection
LS101	h$^+$	*pmk1::KanR*	*sty1:: ura4*$^+$	This work
MI115	h$^-$	*pmp1::KanR*	*pmk1:: ura4*$^+$	Madrid *et al.* 11
MI601	h$^-$	*cdc25-22*	*pmk1::KanR*	Madrid *et al.* 11
MI306	h$^+$	*pek1::KanR*	*pmk1:GFP::leu1*$^+$	Madrid *et al.* 2004
LS102	h$^-$	*rho2::KanR*		This work
LS103	h$^-$	*rho2::KanR*	*pmk1::KanR*	This work
LS104	h$^-$	*pck2::KanR*		This work
LS105	h$^-$	*pck2::KanR*	*pmk1::KanR*	This work
LS106	h$^-$	*atf1:: KanR*		This work
LS107	h$^-$	*atf1:: KanR*	*pmk1::KanR*	This work
LS108	h$^+$	*mbx1:: KanR*		This work
LS109	h$^+$	*mbx1:: KanR*	*pmk1::KanR*	This work
LS110	h$^+$	*atf1:: KanR*	*mbx1:: KanR* *pmk1::KanR*	This work
LS111	h$^+$	*pmk1::KanR*	*pmk1-GFP:: leu1*$^+$	This work
LS112	h$^+$	*pmk1::KanR*	*pmk1 (T186A/Y188F)-GFP:: leu1*$^+$	This work
LS113	h$^+$	*pmk1::KanR*	*pmk1 (T247A/D249A)-GFP:: leu1*$^+$	This work
LS114	h$^+$	*pmk1::KanR*	*pmk1 (R344A/R345A/R355A/R359A/R361A)-GFP:: leu1*$^+$	This work
LS115	h$^+$	*pmk1::KanR*	*pmk1-GFP-CAAX:: leu1*$^+$	This work
LS116	h$^+$	*pmk1::KanR*	*pmk1 (K52E)-GFP-CAAX:: leu1*$^+$	This work
LS117	h$^-$	*pmp1::KanR*	*pmk1::ura4*$^+$ *pmk1-GFP:: leu1*$^+$	This work
LS118	h$^-$	*pmp1::KanR*	*pmk1::ura4*$^+$ *pmk1-GFP-CAAX:: leu1*$^+$	This work
LS119	h$^-$	*rho2::KanR*	*pmk1::KanR* *pmk1-GFP:: leu1*$^+$	This work
LS120	h$^-$	*rho2::KanR*	*pmk1::KanR* *pmk1-GFP-CAAX:: leu1*$^+$	This work
LS121	h$^-$	*pck2::KanR pmk1::KanR*	*pmk1-GFP:: leu1*$^+$	This work
LS122	h$^-$	*pck2::KanR*	*pmk1::KanR* *pmk1-GFP-CAAX:: leu1*$^+$	This work
LS123	h$^-$	*cdc25-22*	*pmk1::KanR* *pmk1-GFP:: leu1*$^+$	This work
LS124	h$^-$	*cdc25-22*	*pmk1::KanR* *pmk1-GFP-CAAX:: leu1*$^+$	This work
LS125	h$^-$	*atf1:: KanR*	*pmk1::KanR* *pmk1-GFP:: leu1*$^+$	This work
LS126	h$^-$	*atf1:: KanR*	*pmk1::KanR* *pmk1-GFP-CAAX:: leu1*$^+$	This work
LS127	h$^+$	*mbx1:: KanR*	*pmk1::KanR* *pmk1-GFP:: leu1*$^+$	This work
LS128	h$^+$	*mbx1:: KanR*	*pmk1::KanR* *pmk1-GFP-CAAX:: leu1*$^+$	This work
LS129	h$^+$	*atf1:: KanR*	*mbx1:: KanR* *pmk1::KanR pmk1-GFP:: leu1*$^+$	This work
LS130	h$^+$	*atf1:: KanR*	*mbx1:: KanR* *pmk1::KanR*	This work
LS131	h$^+$	*pmk1::KanR*	*pmk1-NLS-GFP:: leu1*$^+$	This work
LS132	h$^+$	*pmk1::KanR*	*sty1:: ura4*$^+$ *pmk1-GFP:: leu1*$^+$	This work
LS133	h$^+$	*pmk1::KanR*	*sty1:: ura4*$^+$ *pmk1-GFP-CAAX:: leu1*$^+$	This work
MI702	h$^-$	*pyp2-13myc::ura4* $^+$		Madrid *et al.* 11
LS134	h$^+$	*pmk1::KanR*	*pyp2-13myc::ura4* $^+$	This work
LS135	h$^+$	*pmk1::KanR*	*pmk1-GFP:: leu1*$^+$ *pyp2-13myc::ura4* $^+$	This work
LS136	h$^+$	*pmk1::KanR*	*pmk1-GFP-CAAX:: leu1*$^+$ *pyp2-13myc::ura4* $^+$	This work
LS137	h$^+$	*pmk1::KanR*	*pmk1-GFP-RitC:: leu1*$^+$	This work
MI701	h$^-$	*pyp1-13myc::KanR*		Madrid *et al.* 11
LS138	h$^+$	*pmk1::KanR*	*pmk1-GFP:: leu1*$^+$ *pyp1-13myc::KanR*	This work
LS139	h$^+$	*pmk1::KanR*	*pyp1-13myc::KanR*	This work
MI703	h$^-$	*ptc1-13myc:: KanR*		Madrid *et al.* 11
LS140	h$^+$	*pmk1::KanR*	*pmk1-GFP:: leu1*$^+$ *ptc1-13myc::KanR*	This work
LS141	h$^+$	*pmk1::KanR*	*ptc1-13myc::kanR*	This work

pIL-GFP to construct C-terminal fusions with the GFP tag and containing the *S. pombe leu1*$^+$ gene as a selectable marker. In all cases the resulting plasmids were digested at the unique NruI site within *leu1*$^+$, and the linear fragments were transformed into different *pmk1*Δ genetic backgrounds. Transformants *leu1*$^+$ were obtained, and the correct integration of the fusions was verified by both PCR and Western blot analysis.

The distinct *pmk1*$^+$ mutants were created by the overlap extension method with the use of PCR. The mutagenic primers were as follows: PMKAF-5 (CTGGTTTTATG**G**CGGAGT**T**TGTGGCAA; the nucleotide substitutions are indicated in boldface) and PMKAF-3 (GTTGCCACA**A**ACTCCG**C**CATAAAACCAG) to obtain the *pmk1*-T186A Y188F mutant; PMK4A-5 (GCAAATGAGTTA**GC**C**GC**TGTCATTTTAGATGAAGTTTTAAACTTC**GC**TCAGAAAGTCGCACGCCGCTCTCATC) and PMK4A-3 (GATGAGAGCGGCGT**GC**GACTTTCTGA**GC**GAAGTTTAAAACTTCATCTAAAATGACA**GC**G**GC**TAACTCATTTGC) to obtain the *pmk1*-R344A/R345A/R355A/R359A/R361A mutant; PMKAPA-5 (ATCAACTTGGC**G**CACCTG**C**TGAGGAAACCC) and PMKAPA-3 (GGGTTTCCTCA**G**CAGGTG**C**GCCAAGTTGAT) to obtain the *pmk1*-T247A D249A mutant. In each case the two pairs of PCR products were purified by agarose gel electrophoresis, mixed, and subjected again to PCR with external primers PMKGF-5 and PMKGF-3 (CCTTAGGATCCTTATGGCGATTATCATC), which hybridizes at the 3′ end of *pmk1*$^+$ ORF immediately upstream of the TAA stop codon, and followed by a BamHI site. The PCR products were purified, digested with XbaI and BamHI, and cloned into integrative plasmid pIL-GFP to generate pIL-pmk1(T186A/Y188F):GFP, pIL-pmk1(R344A/R345A/R355A/R359A/R361A):GFP, and pIL-pmk1(T247A/D249A):GFP, respectively. Transformants *leu1*$^+$ were obtained, and the correct integration of the constructs was verified as above. A catalytically inactive version of Pmk1 (K52E mutant) was obtained using the same strategy employing plasmid pIL-pmk1:GFP:C*AAX* as template and the mutagenic primers PMKKE-5 (GGCTGTAGCCATA**G**AAAAAATTACGAAT) and PMKKE-3

(ATTCGTAATTTTTT**C**TATGGCTACAGCC) to obtain plasmid pIL-pmk1(K52E):GFP:C*AAX*.

Stress Treatments and Detection of Activated Pmk1—Experiments to investigate Pmk1 activation under stress were made using log-phase cell cultures (A_{600} = 0.5) growing at 28 °C in YES and supplemented with any of the following compounds: caspofungin (a kind gift from Merck), magnesium chloride (Sigma), potassium chloride (Sigma), or hydrogen peroxide (Sigma). Hypotonic treatment was achieved by growing cells in YES medium plus 0.8 M sorbitol (Sigma) and subsequent transfer to the same medium without polyol. In glucose deprivation studies, cells were grown in YES medium with 7% glucose to an A_{600} = 0.7, recovered by filtration, and resuspended in the same medium without glucose but osmotically equilibrated with 3% glycerol (20). At different times, the cells from 50 ml of culture were harvested by centrifugation at 4 °C and washed with cold PBS buffer, and the yeast pellets were immediately frozen in liquid nitrogen for analysis.

Cell homogenates were prepared under native conditions employing chilled acid-washed glass beads and lysis buffer (10% glycerol, 50 mM Tris-HCl, pH 7.5, 150 mM NaCl, 0.1% Nonidet P-40 plus specific protease and phosphatase inhibitor; Sigma). The lysates were cleared by centrifugation at 13,000 rpm for 15 min, and the proteins were resolved in 10% SDS-PAGE gels, transferred to nitrocellulose filters, and incubated with either polyclonal rabbit anti-GFP (Cell Signaling) or polyclonal rabbit anti-phospho-p42/44 antibodies (Cell Signaling). In cell cycle experiments a rabbit anti-Cdc2 antibody (PSTAIRE; Sigma) was used for loading control. The immunoreactive bands were revealed with anti-rabbit HRP-conjugated secondary antibodies (Sigma) and the ECL detection kit (GE Healthcare). Densitometric quantification of Western blot signals was performed using Molecular Analyst Software (Bio-Rad).

Detection of myc-tagged Fusions—Cell homogenates were prepared under native conditions as indicated above. The cleared lysates were resolved in 8% SDS-PAGE gels, transferred to nitrocellulose filters, and incubated with monoclonal mouse anti-c-myc antibody (clone 9E10, Roche Applied Science). Anti-Cdc2 antibody was used as the loading control.

Northern Blot Analysis—Yeast cells were grown in YES medium to an A_{600} of 0.8 and subjected to the appropriate stress treatment, and volumes of 50 ml of the cultures were recovered at different times. Total RNA preparations were obtained and resolved through 1.5% agarose-formaldehyde gels. Northern (RNA)-hybridization analyses were performed as previously described (21). The probes employed were a 2.1-kbp fragment of the *pyp2*$^+$ gene amplified by PCR with the 5′ oligonucleotide CCGAGAGCGTTTCTTGGA and the 3′ oligonucleotide AAGGGCTTGGAAGCCTGG and a 1-kbp fragment of the *leu1*$^+$ gene amplified with the 5′ oligonucleotide TCGTCGTCTTACCAGGAG and the 3′ oligonucleotide CAACAGCCTTAGTAATAT. Ready-To-Go DNA labeling beads (GE Healthcare) was used for DNA labeling. To establish quantitative conclusions, the level of mRNAs was determined in a PhosphorImager (Molecular Dynamics) and compared with the internal control (*leu1*$^+$ mRNA).

Cell Fractionation—Clarified cell lysates were subjected to centrifugation for 1 h at 45,000 rpm in a Optima TL ultracentrifuge (Beckman Instruments) employing a TLA-100.3 rotor. Once the supernatant was removed, the pellet fractions (P1) were resuspended in lysis buffer plus 7 M urea (final concentration), and incubated at 25 °C for 30 min. The samples were then subjected to ultracentrifugation as above to yield supernatant (S2) and particulate/membrane (P2) fractions. Samples of P1, S2, and P2 fractions were resuspended in SDS/PAGE loading buffer, resolved in 10% SDS-PAGE gels, transferred to nitrocellulose filters, and incubated with anti-GFP antibody.

Plate Assay of Stress Sensitivity for Growth—Wild type and mutant strains of *S. pombe* were grown in YES liquid medium to A_{600} = 0.6. Appropriate dilutions were spotted per duplicate on YES solid medium or in the same medium supplemented with different concentrations of $MgCl_2$, FK506, or caspofungin. Plates were incubated at 28 °C for 3 days and then photographed.

Glucanase Treatments—Cell wall resistance to 1,3-β-glucanase was assayed in different mutants as previously described (11). Cells were grown in YES medium to an A_{600} = 0.6, washed with 10 mM Tris-HCl, pH 7.5, 1 mM EDTA, 1 mM β-mercaptoethanol, and incubated with vigorous shaking at 30 °C in the same buffer supplemented with 100 μg/ml of zymolyase 20T (Seikagaku Corp.). Samples were taken every 15 min, and cell lysis was monitored by measuring A_{600} decay.

Cell Wall Analysis—Labeling and fractionation of cell wall polysaccharides was performed as described previously by Arellano *et al.* (22). In short, exponentially growing cultures of different *S. pombe* strains were supplemented with [U-^{14}C]glucose (0.5 μCi/ml) and incubated for an additional 6 h. Cells were harvested, and total glucose incorporation was monitored by measuring the radioactivity in trichloroacetic acid-insoluble material. Mechanical breakage of cells was done as described for the measurement of the 1–3-β-D-glucan synthase activity. Cell walls were pelleted at 1000 × *g* for 5 min and washed with 5% NaCl 3 times and with 1 mM EDTA 3 times. 100-μl aliquots of the total wall were incubated with 100 units of zymolyase 100T (Seikagaku Corp.) or recombinant 1,3-β-endoglucanase (Quantazyme) for 36 h at 30 °C. Aliquots without enzymes were included as control. Samples were centrifuged, and supernatants and washed pellets were counted separately. The supernatants from zymolyase 100T reaction were considered β-glucan plus galactomannan, and the pellet was α-glucan. The supernatants from the Quantazyme reactions were considered β-glucan, and the pellet was considered α-glucan plus galactomannan.

Fluorescence Microscopy—Images of GFP fusions were taken on a Leica DM 4000B fluorescence microscope with a 100× objective, captured with a cooled Leica DC 300F camera and IM50 software, and then imported and processed with Adobe PhotoShop CS3 (Adobe Systems). Calcofluor white and DAPI were employed for cell wall/septum and nuclei staining, respectively (23). To determine the percentage of multiseptated cells, the number of septated cells was scored in each case ($n > 400$). For vacuole staining, yeast cells were incubated with 5 μM CDCFDA for 10 min as described previously (24) Cell vacuoles were observed with a Leica TCS SP II confocal microscope. The number of vacuoles per cell (a minimum of 50 cells per strain was analyzed) was estimated by collecting images at 1-μm

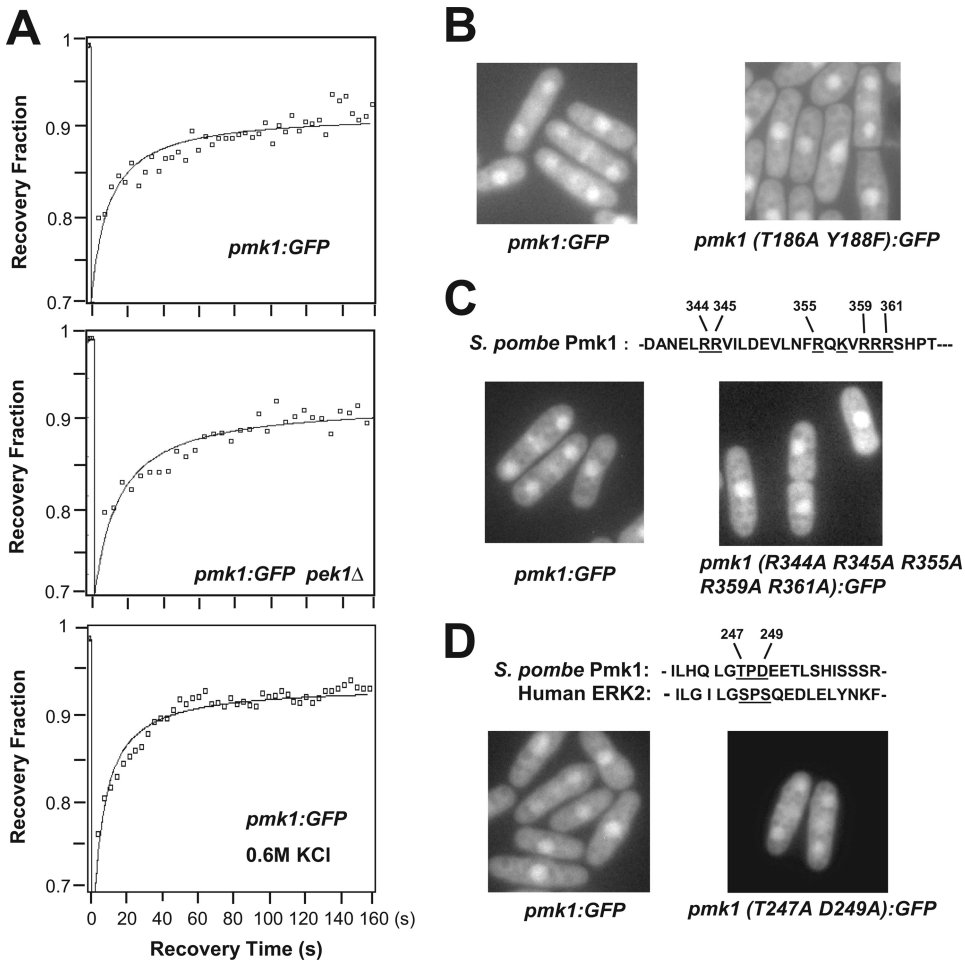

FIGURE 1. **Active and inactive forms of Pmk1 localize into the nucleus in *S. pombe*.** *A*, nuclear recovery of Pmk1-GFP was measured by fluorescence recovery after photobleaching in strains LS111 (control; *upper panel*), MI306 (*pek1*Δ, Pmk1-GFP; *middle panel*), and in LS111 cells subjected to a saline stress with 0.6 M KCl for 20 min (*lower panel*). *B*, shown is fluorescence microscopy of growing cells from strains LS111 (Pmk1-GFP; control) and LS112 (Pmk1(T186A/Y188F)-GFP). *C*, basic residues (*underlined*) that define a putative NLS in Pmk1 amino acid sequence are shown. Fluorescence microscopy of growing cells from strains LS111 (control) and LS114 (Pmk1 (R344A/R345A/R355A/R359A/R361A)-GFP) are shown. *D*, the SPS motif present in ERKs is partially conserved in Pmk1. Fluorescence microscopy of growing cells from strains LS111 (control) and LS113 (Pmk1(T247A/D249A)-GFP).

intervals through the cell (24). Fluorescence recovery after photobleaching experiments were performed using a Deltavision Image Restoration Microscope (Applied Precision/Olympus) and the Softworx software (Applied Precision).

Reproducibility of Results—All experiments were repeated at least three times with similar results. Representative results are shown.

RESULTS

Active and Inactive Forms of Pmk1 Localize into the Nucleus in S. pombe Cells through an Unknown Mechanism—Previous studies indicated that Pmk1 localizes in both the cytoplasm and nucleus as well as in the mitotic spindle and septum during cytokinesis (10). We analyzed Pmk1 dynamics by fluorescence recovery after photobleaching in the nuclear region of strain LS111, expressing a C-terminal-tagged version of Pmk1 fused to GFP under the control of its own promoter. After bleach, Pmk1-GFP recovered into the nucleus at a moderate speed, with visible fluorescence within 15 s after photobleaching ($t_{½}$ = 15.3 ± 1.3 s; n = 10), and showing progressive increase thereafter (Fig. 1*A*, *upper panel*). These results support that Pmk1 MAPK is being continuously transported into the cell nucleus. Notably, nuclear recovery of Pmk1-GFP was not significantly affected in the absence of MAPK kinase Pek1 ($t_{½}$ = 14.1 ± 1.9 s; n = 8; Fig. 1*A*, *middle panel*), suggesting that both the active and inactive forms of the MAPK cross the nuclear membrane at similar rate. We also constructed strain LS112, expressing a version of Pmk1-GFP in which the phosphorylatable threonine 186 and tyrosine 188 residues were changed to alanine and phenylalanine, respectively (Pmk1(T186A/T188F)-GFP). As shown in Fig. 1*B*, the distribution pattern of Pmk1(T186/Y188F)-GFP was not altered as compared with wild type Pmk1-GFP, confirming that dual activating phosphorylation at both threonine 186 and tyrosine 188 is not required for nuclear localization of Pmk1. Consistent with these findings, nuclear recovery of Pmk1-GFP in yeast cells subjected to an osmotic saline stress, which induces a strong MAPK activation (10), remained identical as compared with control cells ($t_{½}$ = 13.9 ± 0.9 s; n = 12; Fig. 1*A*, *lower panel*).

A search for putative sequences required for nuclear accumulation of Pmk1-GFP led to the detection of a potential bipartite NLS at the C-terminal end of Pmk1 (Fig. 1*C*, *upper panel*).

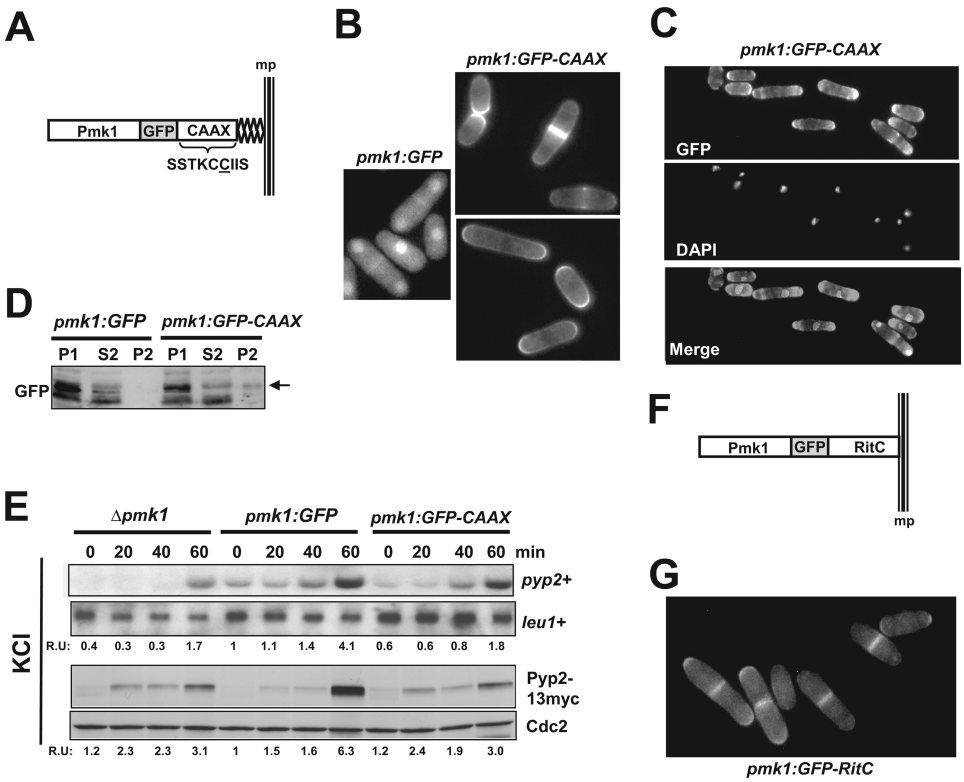

FIGURE 2. **Construction of Pmk1 versions excluded from the nucleus.** *A*, shown is a scheme representing a version of Pmk1 fused at its C terminus to GFP and followed by the addition of the nine terminal residues of Rho2 GTPase. The amino acid sequence SSTKCCIIS incorporates the cysteine residue (*underlined*) that mediates Pmk1 targeting to the plasma membrane. *B*, fluorescence microscopy of growing cells of strain LS115 expressing the Pmk1-GFP-C*AAX* fusion and stained with calcofluor white is shown. *C*, shown is fluorescence microscopy of fixed growing cells of strain LS115 and stained with DAPI. *D*, Western blot analysis of fractionated cell extracts from strains LS111 (Pmk1-GFP) and LS115 is shown. *P1*, pellet fractions. *S2* and *P2* correspond to supernatant and membrane fractions, respectively, obtained from P1 samples treated with 7 M urea (see "Experimental Procedures"). *E*, strains LS134 (*pmk1*Δ, Pyp2–13myc), LS135 (Pmk1-GFP, Pyp2–13myc) (control), and LS136 (Pmk1-GFP-C*AAX* Pyp2–13myc), were grown to mid log-phase and treated with 0.9 M potassium chloride. *pyp2*$^+$ mRNA levels (*upper panel*) were detected by Northern blot analysis after hybridization with ^{32}P-labeled probes for *pyp2*$^+$ and *leu1*$^+$ (loading control) genes. Pyp2 protein levels (*lower panel*) were detected by immunoblotting with anti-c-myc antibody. Anti-Cdc2 antibody was used as the loading control. *F*, shown is a scheme representing a version of Pmk1 fused at its C terminus to GFP and followed by the addition of the C-terminal plasma membrane-targeting domain of the mammalian non-C*AAX* GTPase Rit (RitC). *G*, shown is fluorescence microscopy of growing cells of strain LS137 expressing the Pmk1-GFP-RitC fusion.

To confirm the nature of this sequence as a true nuclear localization signal, we performed site-directed mutagenesis in several basic residues of the motif and analyzed the subsequent effects on Pmk1-GFP localization. However, substitution of arginine residues at positions 344, 345, 355, 359, and 361 with alanine (Pmk1(R344A/R345A/R355A/R359A/R361A)-GFP) did not affect the nuclear localization of the protein fusion (Fig. 1*C*, *left panel*). Recently, it has been shown that ERK2, the metazoan orthologue for Pmk1, contains a three-amino acid domain (SPS) that becomes phosphorylated upon stimulation to induce its nuclear translocation (25). This domain appears only partially conserved in Pmk1 (TPD instead of SPS; Fig. 1*D*). In this context, after replacement of both threonine and aspartic acid residues by alanine (Pmk1(T247A/D249A)-GFP), the nucleocytoplasmic distribution of Pmk1 remained again unchanged (Fig. 1*D*). Moreover, nucleocytoplasmic localization of Pmk1 was not altered in viable α (*imp1*Δ, *cut15-85*)- and β-importin fission yeast mutants (*sal3*Δ, *kap111*Δ, *kap113*Δ, *kap123*Δ, *kap114*Δ, *kap104*Δ, *spcc550.11c*Δ, *spac328.01c*Δ, and *spbp8b7.09c*Δ) (data not shown). As a whole, these findings strongly suggest that neither the nuclear import machinery nor the presence of a canonical NLS- or SPS-like domain are required for nuclear localization of Pmk1 in fission yeast.

Construction of a Pmk1 Version Excluded from the Nucleus—The above results raised questions about the relevance of the nuclear localization of Pmk1 to perform its biological activities. To explore this issue, we constructed strain LS115 expressing a version of Pmk1 fused at its C terminus to GFP and followed by the addition of the nine terminal residues of Rho2 GTPase (amino acids SSTKCCIIS). This amino acid sequence incorporates the cysteine residue (underlined) that, once farnesylated, mediates Rho2 targeting to the plasma membrane (Fig. 2*A*; Ref. 19). Fluorescence microscopy analysis showed that, contrary to Pmk1-GFP, Pmk1-GFP-C*AAX* fusion was completely excluded from the cell nucleus and localized to the plasma membrane (Fig. 2*B*). The membrane-anchored version of Pmk1 appeared mostly around the cell poles and the area surrounding the septum during cytokinesis, thus following a localization pattern quite similar to that previously described for wild type Rho2 (Fig. 2*B*; Ref. 26). Microscopic observation of fixed cells expressing Pmk1-GFP-C*AAX* and stained with DAPI confirmed the absence of MAPK localization at the nuclear region (Fig. 2*C*). Moreover, in contrast to control cells, Western blot analysis allowed detection of the presence of Pmk1-GFP-C*AAX* fusion in urea-treated membrane pellets (*P2*, Fig. 2*D*), further supporting that membrane-targeted Pmk1-GFP-C*AAX* fusion

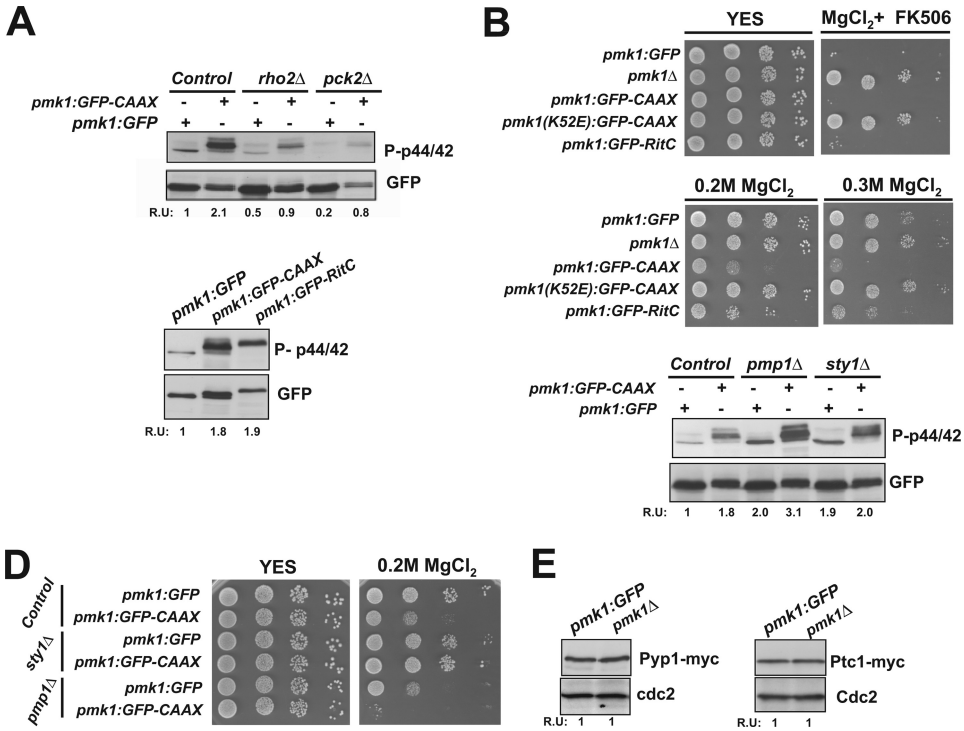

FIGURE 3. **Effect of nuclear exclusion of Pmk1 on chloride homeostasis.** *A*, *upper panel*, cells from strains LS111 (Pmk1-GFP) (control), LS115 (Pmk1-GFP-C*AAX*), LS119 (*rho2*Δ, Pmk1-GFP), LS120 (*rho2*Δ, Pmk1-GFP-C*AAX*), LS121 (*pck2*Δ, Pmk1-GFP), and LS122 (*pck2*Δ, Pmk1-GFP-C*AAX*) were grown in YES medium to mid-log phase. Basal Pmk1 activity was detected by immunoblotting of cell extracts with anti-(phosho-p42/44) antibody, and total Pmk1 was detected with anti-GFP antibody as loading control (*R.U.* indicates relative units). *Lower panel*, cells from strains LS111 (Pmk1-GFP) (control), LS115 (Pmk1-GFP-C*AAX*), and LS137 (Pmk1-GFP-RitC) were grown in YES medium, and basal Pmk1 activity was detected and quantified as described above. *B*, shown are *vic* phenotype and chloride sensitivity assays for strains LS111 (control), MI102 (*pmk1*Δ), LS115, and LS116 (Pmk1(*K52E*)-GFP-C*AAX*; kinase dead). After growth in YES medium, 10^4, 10^3, 10^2, or 10 cells were spotted onto YES plates supplemented with 0.2 M $MgCl_2$ plus 0.5 μg/ml FK506 (*vic*) or with 0.2–0.3 M $MgCl_2$ alone and incubated for 3 days at 28 °C before being photographed. *C*, basal Pmk1 activity in growing cells from strains LS111 (control), LS115, LS117 (*pmp1*Δ, Pmk1-GFP), LS118 (*pmp1*Δ, Pmk1-GFP-C*AAX*), LS132 (*sty1*Δ, Pmk1-GFP), and LS133 (*sty1*Δ, Pmk1-GFP-C*AAX*) was detected as described above. *D*, chloride sensitivity assay for the strains described in C is shown. *E*, strains LS138 (Pmk1-GFP, Pyp1–13myc) and LS139 (*pmk1*Δ, Pyp1–13myc) (*left panel*), and LS140 (Pmk1-GFP, Ptc1–13myc) and LS141 (*pmk1*Δ, Ptc1–13myc) (*right panel*) were grown to mid log-phase, and either Pyp1 or Ptc1 protein levels were detected by immunoblotting with anti-c-myc antibody. Anti-Cdc2 antibody was used as loading control.

is excluded from the cell nucleus. Transcriptional induction of Ptc1, Ptc3, and Pyp2 phosphatases during stress is fully dependent on the SAPK pathway via Sty1-Atf1 (11). However, Pmk1 also targets Atf1 at the cell nucleus and positively regulates this response, as it has been described that increased expression of the above genes (particularly *pyp2*+ mRNA) becomes partially compromised in *pmk1*Δ cells subjected to an osmotic saline stress (14). As compared with control cells (Pmk1-GFP), the induced expression of *pyp2*+ mRNA in osmotic stressed cells was partially reduced in *pmk1*Δ cells (Fig. 2*E*, *upper panel*). Importantly, the reduction of *pyp2*+ gene expression was quite similar both in the *pmk1*Δ mutant and in cells expressing nuclear excluded Pmk1 (Pmk1-GFP-C*AAX* cells; Fig. 2*E*). The same result was obtained after a comparative analysis of Pyp2 protein levels in strains expressing a genomic C-terminal version on *pyp2*+ tagged to a 13myc epitope (Fig. 2*E*; *lower panel*), thus confirming the absence of the Pmk1-GFP-C*AAX* fusion from the nuclear region.

Finally, as an alternative approach for nuclear exclusion of Pmk1, we obtained strain LS137, expressing a version of the MAPK fused at its C terminus to GFP and followed by 62 amino acids corresponding to the C-terminal plasma membrane targeting domain of the mammalian non-C*AAX* GTPase Rit (*RitC*, Fig. 2*F*). This GTPase contains a C-terminal cluster of basic amino acids responsible for membrane association and has been previously employed in fission yeast to target signaling proteins to the plasma membrane (27). As illustrated in Fig. 2*G*, the Pmk1-GFP-RitC fusion remained excluded from the cell nucleus and localized to the plasma membrane, with a pattern very similar to that shown by cells expressing Pmk1-GFP-C*AAX*.

Effect of Nuclear Exclusion of Pmk1 on Chloride Homeostasis—We next determined the basal phosphorylation of Pmk1 in growing cells from strains LS111 (Pmk1-GFP, control) and LS115 (Pmk1-GFP-C*AAX*) by employing an anti-phospho-p44/42 antibody as described previously (10). Fig. 3*A*, *upper panel*, indicates that targeting of Pmk1 to the plasma membrane resulted in the detection of the protein fusion as a slower migrating band in comparison to Pmk1-GFP of control cells. Interestingly, cells expressing membrane-bound Pmk1 displayed a reproducible increase in MAPK basal phosphorylation when compared with control cells (Fig. 3*A*, *upper panel*). A similarly enhanced basal phosphorylation was also observed in cells expressing Pmk1-GFP-RitC fusion (Fig. 3*A*, *lower panel*). Calcineurin and Pmk1 play antagonistic roles in *S. pombe* chloride homeostasis, and either calcineurin inhibition or Pmk1 hyperactivation leads to strong sensitivity to this anion (15). On the contrary, down-regulation of the Pmk1 MAPK cascade allows cells to grow in the presence of 0.2 M $MgCl_2$ and FK506, a specific inhibitor of calcineurin (*vic* phenotype; Ref. 19). As

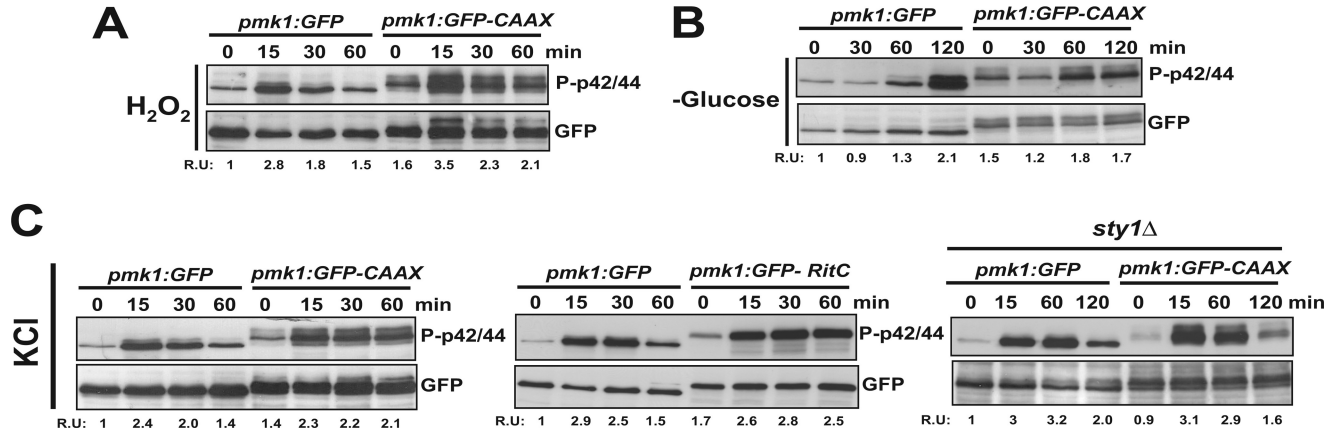

FIGURE 4. **Stress-induced phosphorylation of membrane-targeted Pmk1.** *A*, strains LS111 (Pmk1-GFP; control) and LS115 (Pmk1-GFP-C*AAX*) were grown in YES medium to mid log-phase and treated with 1 mM hydrogen peroxide. At timed intervals either activated or total Pmk1 were detected by immunoblotting with anti-phospho-p42/44 or anti-GFP antibodies, respectively. *B*, both activated and total Pmk1 were detected in strains LS111 and LS115 after glucose depletion. *C*, exponentially growing cells from strains LS111 and LS115 (*left panel*), LS111 and LS137 (Pmk1-GFP-RitC; *middle panel*), or LS132 (*sty1*Δ, Pmk1-GFP) and LS133 (*sty1*Δ, Pmk1-GFP-C*AAX*; *right panel*) were treated with 0.6 M potassium chloride, and both activated and total Pmk1 were detected as described above.

shown in Fig. 3*B*, *upper panel*, and contrary to *pmk1*Δ cells, *S. pombe* strains expressing both membrane-bound Pmk1 versions behaved as the wild type and were unable to grow in rich medium containing 0.2 M $MgCl_2$ and 0.5 μg/ml FK506. Notably, cell sensitivity for growth in medium supplemented with increasing concentrations of $MgCl_2$ was higher in cells expressing either Pmk1-GFP-C*AAX* or Pmk1-GFP-RitC than in Pmk1-GFP or *pmk1*Δ cells (Fig. 3*B*, *lower panel*). Finally, a kinase-dead mutant version of membrane-targeted Pmk1 (Pmk1(*K52E*)-GFP-C*AAX*) displayed the *vic* phenotype and tolerance to chloride anions in a fashion similar to *pmk1*Δ cells (Fig. 3*B*). Taken together, these results indicate that Pmk1 modulates chloride homeostasis outside of the cell nucleus; however, MAPK exclusion from the nuclear region increases its catalytic activity.

Sty1-dependent MAPK phosphatases down-regulate nuclear Pmk1. The above results led us to consider the mechanisms responsible for the enhanced MAPK activity in Pmk1-C*AAX* cells. The addition of the Rho2 farnesylated C*AAX* motif to Pmk1 C-terminal sequence might favor MAPK targeting to membrane locations similar to those of wild type Rho2 (26). Because Rho2 is a positive regulator of the cell integrity pathway (28), the existence of a "Rho2-like" location for Pmk1 might thus result in increased MAPK activation. Deletion of either Rho2 or Pck2 decreased basal Pmk1 phosphorylation in cells expressing Pmk1-GFP-C*AAX* (Fig. 3*A*); however, these values were higher than in *rho2*Δ or *pck2*Δ cells expressing wild type Pmk1-GFP (Fig. 3*A*). Therefore, other factor(s) operating downstream of the MAPK module are likely responsible for the enhanced activity in Pmk1-C*AAX* cells. Hence, an alternative possibility considered was that Pmk1 membrane localization might affect the accessibility of MAPK phosphatases. In this context, previous work has shown that dual-specificity phosphatase Pmp1, tyrosine phosphatase Pyp1, and threonine phosphatase Ptc1 are involved in Pmk1 down-regulation in growing cells (11). Both the high basal Pmk1 phosphorylation and chloride sensitivity in *pmp1*Δ cells were further increased when expressing membrane-tethered Pmk1 (Fig. 3, *C* and *D*), indicating that none of the above phenotypes is related to a lack of MAPK down-regulation by Pmp1. Notably, the increased basal Pmk1 phosphorylation in *sty1*Δ cells, which results from defective synthesis of Pyp1 and Ptc1 phosphatases (11), remained unaffected by the expression of membrane-anchored Pmk1 (Fig. 3*C*). Also, the chloride-sensitive phenotype in Pmk1-C*AAX* cells was suppressed by *sty1*$^+$ deletion (Fig. 3*D*). In this study experiments employing *pyp1*Δ and/or *ptc1*Δ single and/or double mutant strains could not be included as Sty1 hyperactivation perturbs chloride sensitivity in fission yeast (11). Therefore, these results strongly suggest that both the increased Pmk1 phosphorylation and chloride sensitivity in cells expressing membrane-bound Pmk1 are due to the inability of Sty1-regulated phosphatases to down-regulate activated Pmk1 outside the cell nucleus. In agreement with this prediction, basal levels of both Pyp1 and Ptc1 phosphatases (expressed as genomic versions fused to a 13myc epitope) were identical in Pmk1-GFP and *pmk1*Δ cells (Fig. 3*E*).

In fission yeast Pmk1 becomes phosphorylated in response to multiple stresses, including glucose deprivation, oxidative stress, or changes in the osmotic conditions (10). Treatment of growing cells with hydrogen peroxide induced a quick and transient activation of Pmk1 whose kinetics were independent of its subcellular location (Fig. 4*A*). Also, the delayed increase in Pmk1 phosphorylation observed upon glucose withdrawal (10) was quite similar in cells expressing either Pmk1-GFP or Pmk1-GFP-C*AAX* (Fig. 4*B*). As shown in Fig. 4*C*, *left panel*, the Pmk1 phosphorylation in cells expressing either Pmk1-GFP or Pmk1-GFP-C*AAX* became evident 15 min after hypertonic treatment. Nevertheless, cells expressing membrane-bound Pmk1 (either Pmk1-GFP-C*AAX* or Pmk1-GFP-RitC) showed a stress-induced Pmk1 phosphorylation comparatively maintained for longer times (Fig. 4*C*, *left* and *middle panels*). This response might be due to a defective MAPK deactivation by Pyp1, Pyp2, and Ptc1 phosphatases, which are induced by the SAPK pathway and down-regulate Pmk1 activity in response to saline stress (Ref. 11 and Fig. 2*E*). Indeed, the previously described defect in Pmk1 deactivation in *sty1*Δ cells subjected to osmostress (11) was not further enhanced by nuclear exclusion of the

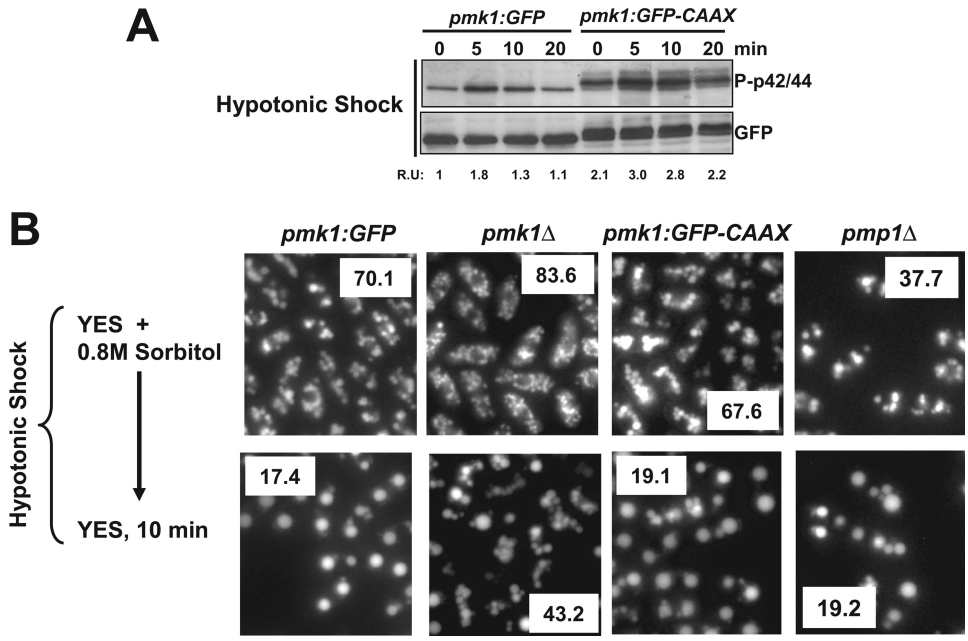

FIGURE 5. **Membrane-tethered Pmk1 promotes vacuole fusion induced during hypotonic stress.** *A*, strains LS111 (Pmk1-GFP; control) and LS115 (Pmk1-GFP-C*AAX*) were grown in YES medium plus 0.8 M sorbitol to mid log-phase and shifted to the same medium without polyol. At timed intervals either activated or total Pmk1 was detected by immunoblotting with anti-phospho-p42/44 or anti-GFP antibodies, respectively. *B*, vacuole fusion is shown. Strains LS111 (Pmk1-GFP; control), MI102 (*pmk1*Δ), LS115 (Pmk1-GFP-C*AAX*), and MI212 (*pmp1*Δ) were grown in YES medium plus 0.8 M sorbitol. Cells were labeled with CDCFDA and resuspended in YES medium, and vacuole size and fusion visualized by fluorescence microscopy. The average number of vacuoles per cell is shown as an insert for control and mutant strains.

MAPK (Fig. 4*C*, *right panel*), indicating that under these conditions Sty1-regulated phosphatases trigger dephosphorylation of activated Pmk1 at the nuclear region.

Membrane-tethered Pmk1 Promotes Vacuole Fusion Induced during Hypotonic Stress—The transfer of wild type *S. pombe* cells from rich medium supplemented with 0.8 M sorbitol to the same medium devoid of stabilizer promotes a hypotonic stress that triggers a very quick and transient Pmk1 phosphorylation (10). As shown in Fig. 5*A*, cells expressing Pmk1-GFP-C*AAX* showed a kinetics of Pmk1 activation by hypotonic stress similar to control cells, except for a modest overall increase in MAPK phosphorylation. A prominent vacuole fusion occurs when *S. pombe* cells are placed in hypotonic medium, and the process appears positively regulated by both Sty1 and Pmk1 MAPKs (24). We labeled the vacuoles of cells exponentially growing in rich medium plus 0.8 M sorbitol with the fluorescent dye CDCFDA. Under these conditions, cells from strains expressing either Pmk1-GFP or Pmk1-GFP-C*AAX* showed a similar average number of vacuoles; however, these were smaller and more abundant in *pmk1*Δ cells (Fig. 5*B*). Remarkably, vacuoles in *pmp1*Δ growing cells were larger and less numerous than in control cells (Fig. 5*B*). These results support that Pmk1 is a positive regulator of vacuole size/number in *S. pombe* and that Pmp1 phosphatase is important for such control. After a few minutes under hypotonic stress, cell vacuoles from strains expressing either Pmk1-GFP (wild type, *pmp1*Δ) or Pmk1-GFP-C*AAX* fused rapidly and to a similar extent, whereas, contrarily, cells from *pmk1*Δ strain showed a partial defect in vacuole fusion (Fig. 5*B*). Therefore, the functional role of Pmk1 during vacuole fusion is not linked to its presence into the nucleus.

Cell Separation Defect in Cells Expressing a Pmk1 Version Excluded from the Nucleus—A typical feature of null mutants in members of the MAPK cell integrity pathway is the presence of multiseptated cells, indicating that Pmk1 is positively involved in the regulation of cell separation (5, 6). Consequently, we analyzed the effect of nuclear exclusion of Pmk1 on this process. As shown in Fig. 6, *A* and *B*, when compared with control cells, we observed a small increase in the percentage of septation in asynchronous-growing cultures of cells expressing membrane-tethered Pmk1 in both minimal medium and YES medium supplemented with 1 M sorbitol. However, and contrary to *pmk1*Δ cells or to cells with a kinase-dead membrane-targeted Pmk1, no significant multiseptation was detected in cells expressing either Pmk1-GFP-C*AAX* or Pmk1-GFP-RitC (Fig. 6, *A* and *B*). We previously reported that Pmk1 dual phosphorylation oscillates through the cell cycle, peaking at cell separation during G_1-S transition in coincidence with cytokinesis (Fig. 6*C*, *upper panel*; Ref. *vic* 11). Interestingly, expression of membrane-bound Pmk1 did not have a noticeable effect on the kinetics of Pmk1 phosphorylation, although we detected the presence of some multiseptated cells during the second division cycle (Fig. 6*C*, *middle panel*). Such phenotype, however, was much less severe than in *pmk1*Δ cells, where as described earlier ~15–20% cells are unable to complete cytokinesis (Fig. 6*C*, *lower panel*; Ref. 11).

Cell Wall Integrity Is Partially Compromised in Fission Yeast Cells Expressing Nuclear-excluded Pmk1—Deletion of genes encoding members of the cell integrity MAPK pathway causes hypersensitivity to β-glucanases (6, 9, 10), indicating cell wall defects. We analyzed the lytic sensitivity in exponentially growing cultures of different mutants after treatment with the β-glu-

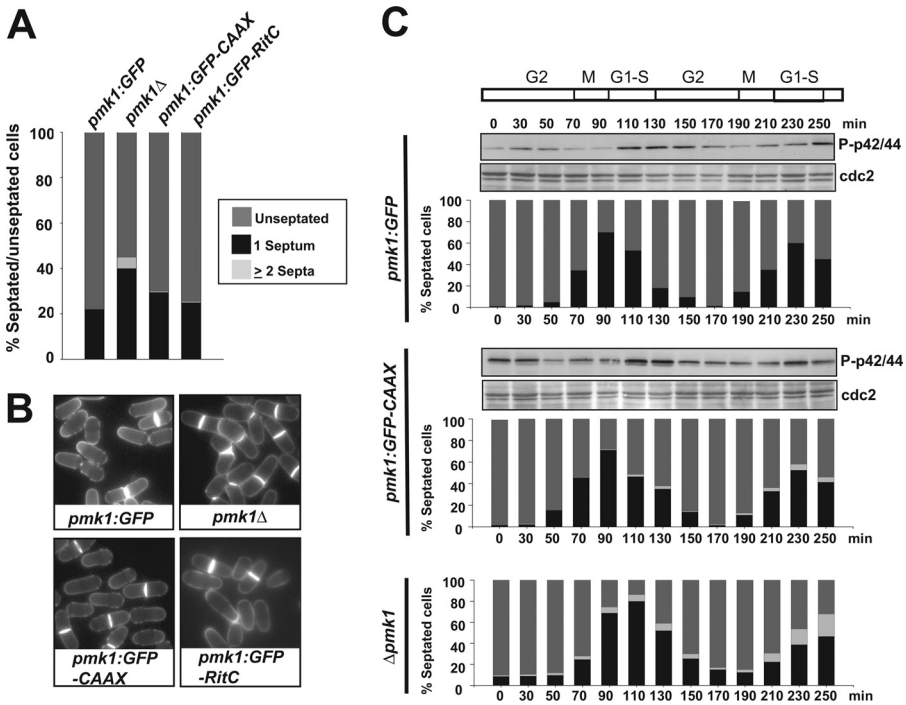

FIGURE 6. **Cell separation defect in cells expressing a Pmk1 version excluded from the nucleus.** *A*, strains LS111 (Pmk1-GFP; Control), MI102 (*pmk1*Δ), LS115 (Pmk1-GFP-C*AAX*), and LS137 (Pmk1-GFP-RitC) were grown in YES medium plus 0.8 M sorbitol to mid log-phase, and the percentage of unseptated/septated cells in cultures was determined by fluorescence microscopy after cell staining (n≥400) with calcofluor white. *B*, representative cells from the strains described above as observed by fluorescence microscopy. *C*, cells from strains LS123 (*cdc25-22*, Pmk1-GFP), LS124 (*cdc25-22*, Pmk1-GFP-C*AAX*), and MI601 (*cdc25-22*, *pmk1*Δ) were grown to A_{600} = 0.3 at 25 °C, shifted to 37 °C for 3.5 h, and then released from the growth arrest by transfer back to 25 °C. Aliquots were taken at different time intervals, and activated Pmk1 was detected by immunoblotting with anti-phospho-p42/44 antibodies. Anti-Cdc2 antibody was employed as loading control. Percentage of unseptated, septated, and multiseptated cells at each time point is shown as described in *A*.

canase complex zymolyase 20T. In contrast to control cells, cells lacking Pmk1 displayed higher sensitivity to β-1,3-glucanase, as previously described (Fig. 7*A*; Refs. 5, 6, and 9). Notably, *S. pombe* cells expressing membrane-bound Pmk1 (either Pmk1-GFP-C*AAX* or Pmk1-GFP-RitC cells) were clearly more sensitive than control cells, although not as much as single *pmk1*Δ mutant cells (Fig. 7*A*). To further examine the role of Pmk1 localization in the regulation of cell wall biosynthesis, we also analyzed the cell wall composition in *pmk1*Δ mutant cells and in strains expressing either Pmk1-GFP or Pmk1-GFP-C*AAX*. As shown in Fig. 7*B*, compared with control cells, both *pmk1*Δ and Pmk1-GFP-C*AAX* cells displayed an overall increase (~5%) in the amount of glucose incorporated in total cell wall. In addition, in *pmk1*Δ and Pmk1-GFP-C*AAX* cells there was an increased amount of α-glucan (18 and 7%, respectively) and galactomanan (25 and 50%, respectively) as compared with control cells (Fig. 7*B*). Thus, these findings suggest that the cell integrity MAPK pathway negatively affects the synthesis of α-glucan and galactomanan in the cell wall of fission yeast and that the normal process relies in part on the presence of Pmk1 at the cell nucleus. We also noticed that both Pmk1-GFP-C*AAX* and Pmk1-GFP-RitC cells were more sensitive for growth in the presence of caspofungin (a potent β-glucan synthase inhibitor) than control cells, although not as much as the *pmk1*Δ mutant (Fig. 7*C*). Pmk1 activation in response to cell wall stress induced by caspofungin was similar in Pmk1-GFP-C*AAX* cells (Fig. 7*D*). Nevertheless, in strong contrast with the results on chloride homeostasis (Fig. 2*C*), Sty1 deletion did not suppress the increased caspofungin sensitivity observed in cells with nuclear-excluded Pmk1-GFP-C*AAX* (Fig. 7*D*), thus corroborating the interpretation that this phenotype is not due to an enhanced MAPK activity. Taken together, the above results support the notion that nuclear Pmk1 might play a transcriptional role in response to alterations in cell wall integrity.

The transcription factor Atf1, which is the main target of Sty1 in fission yeast, is known to be specifically activated by Pmk1 to regulate gene expression in response to cell wall stress (14). However, as shown in Fig. 7*E*, the caspofungin sensitivity in cells expressing Pmk1-GFP-C*AAX* was slightly enhanced in absence of Atf1, suggesting that this response is unrelated to a defective control of Atf1 function. Surprisingly, we observed that deletion of the gene encoding MADS box-type transcription factor Mbx1, which has been involved together with Atf1 in the induced expression of the glycosylphosphatidylinositol-anchored cell surface protein Ecm33 (29), partially suppressed the caspofungin sensitivity in Pmk1-GFP-C*AAX* cells (Fig. 7*E*). Therefore, these findings indicate that Pmk1-dependent regulation of Mbx1 activity at the cell nucleus is an important factor for adequate transcriptional response to cell wall stress.

Biological Relevance of Increased Nuclear Localization of Pmk1—We focused on a complementary approach to evaluate the biological significance of the nuclear localization of Pmk1 by constructing a *S. pombe* strain expressing a version of Pmk1 fused at its C terminus to the NLS of the SV-40 virus large T antigen (PKKKRKV) followed by GFP (Pmk1-NLS-GFP; Fig. 8*A*). Pmk1-NLS-GFP appears to be mostly confined to the cell nucleus, although some fluorescence was still detected in the cell separation area and the cytoplasm (Fig. 8*A*). Both basal and

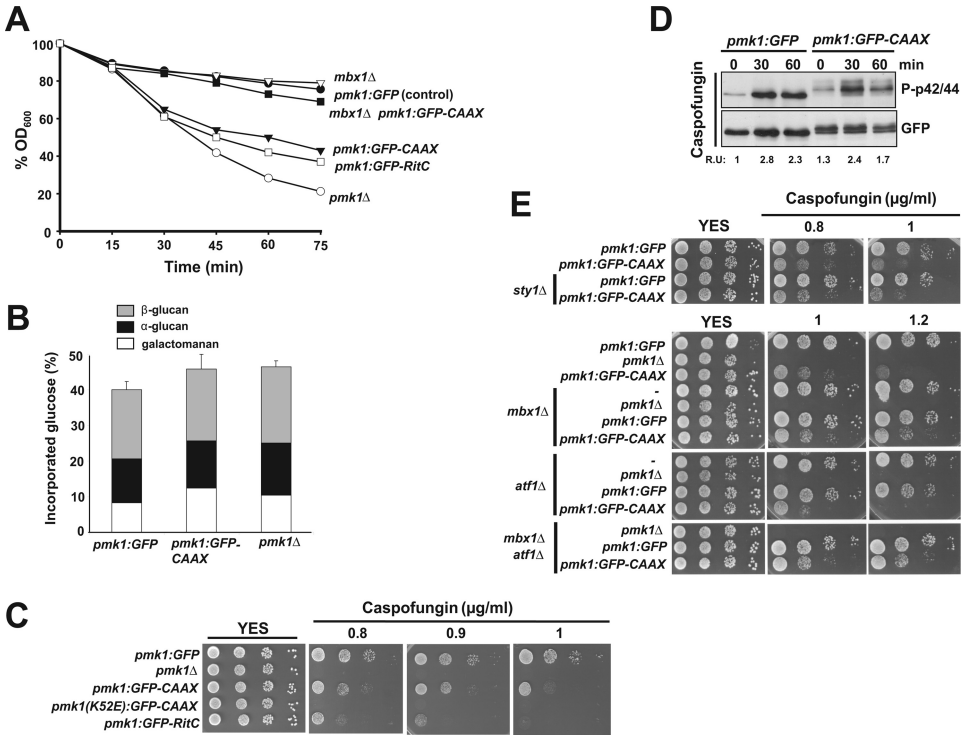

FIGURE 7. **Cell wall integrity is partially compromised in cells expressing a nuclear-excluded version of Pmk1.** *A*, strains LS111 (Pmk1-GFP; control), MI102 (*pmk1*Δ), LS115 (Pmk1-GFP-*CAAX*), LS137 (Pmp1-GFP-RitC), LS127 (*mbx1*Δ, Pmk1-GFP), and LS128 (*mbx1*Δ, Pmk1-GFP-*CAAX*) were grown in YES medium (A_{600} = 0.5) and assayed for β-glucanase sensitivity. Cell lysis was monitored by measuring decay in A_{600} for different incubation periods. Results shown are the mean value of three independent experiments. *B*, cell wall composition of strains LS111 (control), MI102, and LS115 is shown. Strains were grown in YES medium at 32 °C, and [^{14}C]glucose was added 6 h before harvesting. Values shown are the mean of three independent experiments with duplicate samples, and *error bars* represent S.D. for total carbohydrate values. *C*, caspofungin sensitivity assays for strains LS111 (Pmk1-GFP; control), MI102 (*pmk1*Δ), LS115 (Pmk1-GFP-*CAAX*), LS116 (Pmk1(*K52E*)-GFP-*CAAX*; kinase dead), and LS137 (Pmk1-GFP-RitC) are shown. After growth in YES medium, 10^4, 10^3, 10^2, or 10 cells were spotted onto YES plates supplemented with 0.8, 1.0, or 1.2 μg/ml caspofungin and incubated for 3 days at 28 °C before being photographed. *D*, strains LS111 (Pmk1-GFP; control) and LS115 (Pmk1-GFP-*CAAX*) were grown in YES medium to mid log-phase and treated with 1 μg/ml caspofungin. At timed intervals either activated or total Pmk1 was detected by immunoblotting with anti-phospho-p42/44 or anti-GFP antibodies, respectively. *E*, shown are caspofungin sensitivity assays for strains LS111, LS115, LS132 (*sty1*Δ, Pmk1-GFP), LS133 (*sty1*Δ, Pmk1-GFP-*CAAX*), MI102, LS108 (*mbx1*Δ), LS109 (*mbx1*Δ *pmk1*Δ), LS127 (*mbx1*Δ, Pmk1-GFP), LS128 (*mbx1*Δ, Pmk1-GFP-*CAAX*), LS106 (*atf1*Δ), LS107 (*atf1*Δ *pmk1*Δ), LS125 (*atf1*Δ, Pmk1-GFP), LS126 (*atf1*Δ, Pmk1-GFP-*CAAX*), LS110 (*mbx1*Δ *atf1*Δ *pmk1*Δ), LS129 (*mbx1*Δ *atf1*Δ, Pmk1-GFP), and LS130 (*mbx1*Δ *atf1*Δ, Pmk1-GFP-*CAAX*).

salt stress-induced Pmk1 activation were partially compromised in Pmk1-NLS-GFP cells as compared with control cells (Fig. 8*B*). Importantly, enhanced nuclear accumulation of Pmk1 resulted in a *vic* phenotype, which was not as strong as in *pmk1*Δ cells (Fig. 8*C*). In comparison to control cells, Pmk1-NLS-GFP cells displayed a less marked sensitivity for growth in the presence of caspofungin than those expressing membrane-tethered Pmk1 (Fig. 8*D*). These findings reinforce the results described above and are congruent with the idea that nuclear localization of Pmk1 is important for accurate control of both chloride homeostasis and cell wall integrity.

DISCUSSION

Nuclear localization of MAPKs is essential for proper function and subsequent regulation of distinct cellular processes. However, regardless of the existence of a classical pathway for nuclear import of proteins, many of these effectors, including some ERKs, do not contain the canonical NLS, and mechanisms for their nuclear targeting remain unknown (25). In agreement with these precedents, results presented in this work strongly suggest that the constitutive nuclear localization of Pmk1 in fission yeast is independent on its phosphorylation status. In addition, our observations that MAPK localization remained unchanged in cells expressing a Pmk1 mutant lacking a putative NLS signal or in the absence of known α- and β-importins points to the fact that neither the presence of a canonical NLS nor the function of the nuclear import machinery is involved in its nuclear location. Nuclear translocation of ERKs can occur either by a passive diffusion or by active transport (30, 31). In budding yeast it has been reported that β-karyopherin Kap95 is responsible for nuclear import of the Pmk1 ortholog Slt2 MAPK (32). Unfortunately, deletion of the Kap95 ortholog (SAPC1B1.03c) is lethal in fission yeast, and therefore, its role in Pmk1 nuclear localization has not been evaluated. Nevertheless, Pmk1 MAPK localization was unaffected in mutants lacking non-essential β-karyopherins (9 of 12 present in fission yeast genome), although the possibility still remains that Pmk1 might use multiple importins for *in vivo* nuclear location. Contrary to the findings described here, Sty1, which is the core MAPK of the SAPK pathway in fission yeast, localizes mainly in the cytoplasm in unstressed cells, whereas binding and phosphorylation by MAPK kinase Wis1 triggers Sty1 transport to the nucleus upon stress (33). Moreover, the Ran GDP/GTP exchange factor Pim1 is important for Sty1 nuclear accumulation under stress, and exportin Crm1 participates in its nuclear exclusion (34). Interestingly, phosphorylation of a conserved

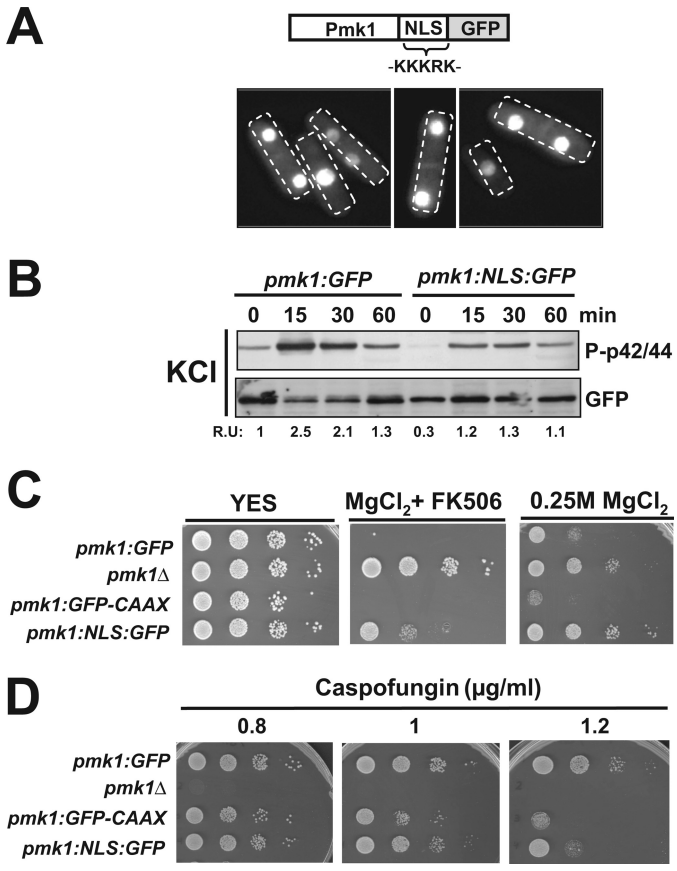

FIGURE 8. **Biological relevance of increased nuclear localization of Pmk1.** *A*, shown is a scheme representing a version of Pmk1 fused at its C terminus to the SV40 nuclear localization signal followed by GFP epitope and growing cells of strain LS131 expressing the Pmk1-NLS-GFP fusion as seen by fluorescence microscopy. *B*, exponentially growing cells of strains LS111 (Pmk1-GFP, control) and LS131 (Pmk1-NLS-GFP) were treated with 0.6 M potassium chloride, and both activated and total Pmk1 were detected by immunoblotting with anti-phospho-p42/44 or anti-GFP antibodies, respectively. *C*, *vic* phenotype and chloride sensitivity assays for strains LS111 (control), MI102 (*pmk1*Δ), LS115, and LS131 are shown. After growth in YES medium, 10^4, 10^3, 10^2, or 10 cells were spotted onto YES plates supplemented with 0.2 M $MgCl_2$ plus 0.5 µg/ml FK506 (*vic*), or 0.25 M $MgCl_2$ alone and incubated for 3 days at 28 °C before being photographed. *D*, shown are caspofungin sensitivity assays for the strains described in *C*.

SPS motif present in ERKs has been described as responsible for both active and passive MAPK nuclear translocation (25). However, mutation in the partially conserved motif present in Pmk1 did not impair its nuclear localization. Hence, a yet unknown mechanism appears responsible for Pmk1 nuclear targeting in fission yeast.

An important result obtained in our work is that fission yeast cells expressing a nuclear excluded, membrane-bound versions of Pmk1 can recapitulate many of the biological functions previously assigned to wild type (nucleo-cytoplasmic) Pmk1. Among these, we analyzed the regulation of chloride homeostasis, vacuole fusion during hypotonic stress, and cellular separation (5, 6, 15, 11). However, our findings also show that nucleo-cytoplasmic shuffling of activated Pmk1 is important for proper spatial and temporal down-regulation of its biological activity and that this subtle regulatory mechanism is performed at the nuclear region by specific MAPK phosphatases. This is particularly clear during the control of chloride homeostasis, which relies primarily on active extranuclear Pmk1. However, MAPK targeting to the cell nucleus is also important for a fine-tuning regulation of this process, as evidenced by the fact that although both basal Pmk1 phosphorylation and chloride sensitivity are increased in cells expressing membrane-bound Pmk1, forced nuclear targeting of Pmk1 (Pmk1-NLS-GFP mutant) results only in a moderate *vic* phenotype that is associated with down-regulation of Pmk1 activity. On the other hand, Pmk1-dependent regulation of cell separation mostly operates in way independent on its localization at the nuclear region, giving support to early predictions suggesting that this process might be performed by activated MAPK specifically located at the division area (10). Nonetheless, the existence of a weak separation defect in cells expressing membrane-tethered Pmk1 strongly suggests that, similar to chloride homeostasis, MAPK down-regulation in the cell nucleus defines the precise outcome of this cellular event. Fission yeast cells lacking Pmp1 phosphatase display both altered Pmk1 phosphorylation during cell cycle and a strong cell separation defect (11). Hence, the overall increase in phosphorylation during cell cycle prompted by nuclear exclusion of Pmk1 appears to be the reason for the subtle separation defect observed in cells expressing membrane-targeted Pmk1. Interestingly, the nuclear absence of Pmk1 did not alter its positive role in the maintenance of vacuole size/number and induced fusion under hypotonic stress, implying that nuclear regulation of Pmk1 activity is restricted to specific biological events.

The known phosphatases, which can inactivate Pmk1 (Pmp1, Pyp1, Pyp2, and Ptc1) are nucleo-cytoplasmic proteins (35) and, therefore, good candidates to specifically down-regulate this MAPK at the cell nucleus. Evidence presented in this work suggest that such a role is performed in growing cells and in response to specific stresses (*i.e.* osmostress) by the Sty1-regulated phosphatases Pyp1, Pyp2, and/or Ptc1, whereas dual specificity phosphatase Pmp1 down-regulates cytoplasmic Pmk1 during vegetative growth. This suggestion is based on the fact that, contrary to *pmp1*Δ cells, nuclear exclusion of Pmk1 did not enhance the high basal MAPK phosphorylation or the defective Pmk1 dephosphorylation in growing and osmostressed *sty1*Δ cells, respectively. This scenario is somehow similar to the model described in budding yeast where tyrosine phosphatase Ptp2 (Pyp1 homologue) is the main negative regulator of nuclear-activated forms of MAPKs Hog1 (Sty1 ortholog) and Slt2 (36). On the contrary, Ptp3 tyrosine phosphatase (Pyp2 homolog) down-regulates both Hog1 and Slt2 at the cytoplasm (36). Importantly, whereas Ptp2 acts as a nuclear anchor for both Hog1 and Slt2 and Ptp3 is its cytoplasmic counterpart, Pmk1 localization in fission yeast is not affected by deletion of Sty1-regulated phosphatases (11). Thus, opposite to other eukaryotic organisms including budding yeast, fission yeast MAPK phosphatases do not act as nuclear anchors for Pmk1. On the other hand, the possibility that the high MAPK activity observed in cells expressing nuclear-excluded Pmk1 could be caused by the lack of proper adaptation rather than an increased activity *per se* or the deficient accessibility by protein phosphatases should also be considered.

Although the role of Pmk1 in maintaining cell wall integrity is partially independent on its nuclear location, we also found that fission yeast cells expressing membrane-tethered Pmk1

display altered cell wall composition and increased sensitivity to cell wall-degrading compounds. In striking contrast to chloride homeostasis, these differential defects do not result from defective MAPK down-regulation at the cell nucleus, thus suggesting that Pmk1-mediated transcriptional activity might play a role in response to cell wall stress. In this framework, there is a report describing that Pmk1 can phosphorylate Atf1 during cell wall damage (14), thus making this transcription factor a good candidate for enhanced gene expression and cell survival under these conditions. We found, however, that caspofungin sensitivity in *atf1*Δ cells was lower and additive to that of cells expressing nuclear-excluded Pmk1, indicating that other element(s) may be involved in this response. This finding may be not surprising, as the number of identified genes whose expression is induced under stress in a Pmk1-Atf1-dependent fashion is currently rather limited (29, 37).[5] The demonstration that cell wall defects in cells expressing membrane-anchored Pmk1 were in part alleviated by simultaneous deletion of Mbx1 are intriguing. MADS box-like protein Mbx1 together with forkhead-like proteins Sep1 and Fkh2 are part of the pombe cell cycle box binding factor transcription factor complex that is involved in the expression of a specific set of genes during the M-G_1 phase of the cell cycle (38). Moreover, Mbx1 phosphorylation is controlled by the polo-like kinase Plo1 and the Cdc14p-like phosphatase Clp1p (Flp1p) (38, 39). The finding that Mbx1 regulates together with Atf1 the expression of the *ecm33*+ gene in a Pmk1 dependent fashion has pointed to Plo1 and Pmk1 kinases as coordinately regulating cell cycle and/or cell integrity signaling via the phospho-regulation of Mbx1 activity (29). In this respect, our results suggest that whereas Pmk1 positively regulates Mbx1 transcriptional activity in the cell nucleus, lack of MAPK regulation at this cell compartment might convert Mbx1 in a transcriptional repressor. Further studies will be needed to clarify the functional relation between the Pmk1 cell integrity pathway and Mbx1. Whatever the case may be, the contribution of extra-nuclear Pmk1 during this response appears at least as relevant as its role in the cell nucleus given the intermediate cell wall defects displayed by either Pmk1-C*AAX* or Pmk1-RitC cells in comparison to both control and a Pmk1-less mutant. In *Saccharomyces cerevisiae* it has been shown that nuclear Hog1-mediated transcriptional response is not necessary for hyperosmotic stress resistance (40). This observation and the results presented here suggest that MAPK-controlled transcriptional programs are much less relevant during cell survival against stress than initially thought.

In conclusion, our study on the differential activities of MAPK Pmk1 attached to the plasma membrane shows that in fission yeast most of the functions driven by the cell integrity pathway are carried out independently of the Pmk1 presence into the nucleus. Although nuclear Pmk1 might partially regulate cell wall integrity at a transcriptional level by positively targeting Atf1 and Mbx1, constitutive localization at this compartment allows MAPK down-regulation by specific phosphatases, thus modulating its overall biological activity. These results highlight the importance of the spatial control of MAPK activity, a feature likely shared with higher eukaryotes.

[5] L. Sánchez-Mir, A. Franco, M. Madrid, J. Vicente-Soler, M. A. Villar-Tajadura, T. Soto, P. Pérez, M. Gacto, and J. Cansado, unpublished results.

Acknowledgments—We thank T. Toda (London Research Institute, Cancer Research UK) and P. Nurse (Rockefeller University) for the kind supply of yeast strains, J. B. Millar (University of Warwick) for generous access to the Deltavision system, and F. Garro for technical assistance.

REFERENCES

1. Kim, E. K., and Choi, E. J. (2010) Pathological roles of MAPK signaling pathways in human diseases. *Biochim. Biophys. Acta* **1802,** 396–405
2. Qi, M., and Elion, E. A. (2005) MAP kinase pathways. *J. Cell Sci.* **118,** 3569–3572
3. Krisak, L., Strich, R., Winters, R. S., Hall, J. P., Mallory, M. J., Kreitzer, D., Tuan, R. S., and Winter, E. (1994) SMK1, a developmentally regulated MAP kinase, is required for spore wall assembly in *Saccharomyces cerevisiae*. *Genes Dev.* **8,** 2151–2161
4. Shiozaki, K., and Russell, P. (1995) Cell cycle control linked to extracellular environment by MAP kinase pathway in fission yeast. *Nature* **378,** 739–743
5. Toda, T., Dhut, S., Superti-Furga, G., Gotoh, Y., Nishida, E., Sugiura, R., and Kuno, T. (1996) The fission yeast pmk1+ gene encodes a novel mitogen-activated protein kinase homolog that regulates cell integrity and functions coordinately with the protein kinase C pathway. *Mol. Cell. Biol.* **16,** 6752–6764
6. Zaitsevskaya-Carter, T., and Cooper, J. A. (1997) Spm1, a stress-activated MAP kinase that regulates morphogenesis in *S. pombe*. *EMBO J.* **16,** 1318–1331
7. Pérez, P., and Cansado, J. (2010) Cell integrity signaling and response to stress in fission yeast. *Curr. Protein Pept. Sci.* **11,** 680–692
8. Sugiura, R., Toda, T., Dhut, S., Shuntoh, H., and Kuno, T. (1999) The MAPK kinase Pek1 acts as a phosphorylation-dependent molecular switch. *Nature* **399,** 479–483
9. Loewith, R., Hubberstey, A., and Young, D. (2000) Skh1, the MEK component of the mkh1 signaling pathway in *Schizosaccharomyces pombe*. *J. Cell Sci.* **113,** 153–160
10. Madrid, M., Soto, T., Khong, H. K., Franco, A., Vicente, J., Pérez, P., Gacto, M., and Cansado, J. (2006) Stress-induced response, localization, and regulation of the Pmk1 cell integrity pathway in *Schizosaccharomyces pombe*. *J. Biol. Chem.* **281,** 2033–2043
11. Madrid, M., Núñez, A., Soto, T., Vicente-Soler, J., Gacto, M., and Cansado, J. (2007) Stress-activated protein kinase-mediated down-regulation of the cell integrity pathway mitogen-activated protein kinase Pmk1p by protein phosphatases. *Mol. Biol. Cell* **18,** 4405–4419
12. Sugiura, R., Kita, A., Shimizu, Y., Shuntoh, H., Sio, S. O., and Kuno, T. (2003) Feedback regulation of MAPK signaling by an RNA-binding protein. *Nature* **424,** 961–965
13. Satoh, R., Morita, T., Takada, H., Kita, A., Ishiwata, S., Doi, A., Hagihara, K., Taga, A., Matsumura, Y., Tohda, H., and Sugiura, R. (2009) Role of the RNA-binding protein Nrd1 and Pmk1 mitogen-activated protein kinase in the regulation of myosin mRNA stability in fission yeast. *Mol. Biol. Cell* **20,** 2473–2485
14. Takada, H., Nishimura, M., Asayama, Y., Mannse, Y., Ishiwata, S., Kita, A., Doi, A., Nishida, A., Kai, N., Moriuchi, S., Tohda, H., Giga-Hama, Y., Kuno, T., and Sugiura, R. (2007) Atf1 is a target of the mitogen-activated protein kinase Pmk1 and regulates cell integrity in fission yeast. *Mol. Biol. Cell* **18,** 4794–4802
15. Sugiura, R., Toda, T., Shuntoh, H., Yanagida, M., and Kuno, T. (1998) pmp1+, a suppressor of calcineurin deficiency, encodes a novel MAP kinase phosphatase in fission yeast. *EMBO J.* **17,** 140–148
16. Moreno, S., Klar, A., and Nurse, P. (1991) Molecular genetic analysis of fission yeast *Schizosaccharomyces pombe*. *Methods Enzymol.* **194,** 795–823
17. Soto, T., Beltrán, F. F., Paredes, V., Madrid, M., Millar, J. B. A., Vicente-Soler, J., Cansado, J., and Gacto, M. (2002) Cold induces stress-activated

protein kinase-mediated response in the fission yeast *Schizosaccharomyces pombe*. *Eur. J. Biochem.* **269,** 5056–5065
18. Bähler, J., Wu, J. Q., Longtine, M. S., Shah, N. G., McKenzie, A., 3rd, Steever, A. B., Wach, A., Philippsen, P., and Pringle, J. R. (1998) Heterologous modules for efficient and versatile PCR-based gene targeting in *Schizosaccharomyces pombe*. *Yeast* **14,** 943–951
19. Ma, Y., Kuno, T., Kita, A., Asayama, Y., and Sugiura, R. (2006) Rho2 is a target of the farnesyltransferase Cpp1 and acts upstream of Pmk1 mitogen-activated protein kinase signaling in fission yeast. *Mol. Biol. Cell* **17,** 5028–5037
20. Madrid, M., Soto, T., Franco, A., Paredes, V., Vicente, J., Hidalgo, E., Gacto, M., and Cansado, J. (2004) A cooperative role for Atf1 and Pap1 in the detoxification of the oxidative stress induced by glucose deprivation in *Schizosaccharomyces pombe*. *J. Biol. Chem.* **279,** 41594–41602
21. Núñez, A., Franco, A., Madrid, M., Soto, T., Vicente, J., Gacto, M., and Cansado, J. (2009) Role for RACK1 orthologue Cpc2 in the modulation of stress response in fission yeast. *Mol. Biol. Cell* **20,** 3996–4009
22. Arellano, M., Duran, A., and Perez, P. (1997) Localization of the *Schizosaccharomyces pombe* rho1p GTPase and its involvement in the organization of the actin cytoskeleton. *J. Cell Sci.* **110,** 2547–2555
23. Alfa, C., Fantes, P., Hyams, J., Mcleod, M., and Warbrick, E. (1993) *Experiments with Fission Yeast*, pp. 16–24, Cold Spring Harbor Laboratory Press, Cold Spring Harbor, NY
24. Bone, N., Millar, J. B., Toda, T., and Armstrong, J. (1998) Regulated vacuole fusion and fission in *Schizosaccharomyces pombe*. An osmotic response dependent on MAP kinases. *Curr. Biol.* **8,** 135–144
25. Chuderland, D., Konson, A., and Seger, R. (2008) Identification and characterization of a general nuclear translocation signal in signaling proteins. *Mol. Cell* **31,** 850–861
26. Hirata, D., Nakano, K., Fukui, M., Takenaka, H., Miyakawa, T., and Mabuchi, I. (1998) Genes that cause aberrant cell morphology by overexpression in fission yeast. A role of a small GTP-binding protein Rho2 in cell morphogenesis. *J. Cell Sci.* **111,** 149–159
27. Onken, B., Wiener, H., Philips, M. R., and Chang, E. C. (2006) Compartmentalized signaling of Ras in fission yeast. *Proc. Natl. Acad. Sci. U.S.A.* **103,** 9045–9050
28. Barba, G., Soto, T., Madrid, M., Núñez, A., Vicente, J., Gacto, M., and Cansado, J. (2008) Activation of the cell integrity pathway is channeled through diverse signaling elements in fission yeast. *Cell. Signal.* **20,** 748–757
29. Takada, H., Nishida, A., Domae, M., Kita, A., Yamano, Y., Uchida, A., Ishiwata, S., Fang, Y., Zhou, X., Masuko, T., Kinoshita, M., Kakehi, K., and Sugiura, R. (2010) The cell surface protein gene ecm33+ is a target of the two transcription factors Atf1 and Mbx1 and negatively regulates Pmk1 MAPK cell integrity signaling in fission yeast. *Mol. Biol. Cell* **21,** 674–685
30. Adachi, M., Fukuda, M., and Nishida, E. (1999) Two co-existing mechanisms for nuclear import of MAP kinase. Passive diffusion of a monomer and active transport of a dimer. *EMBO J.* **18,** 5347–5358
31. Yazicioglu, M. N., Goad, D. L., Ranganathan, A., Whitehurst, A. W., Goldsmith, E. J., and Cobb, M. H. (2007) Mutations in ERK2 binding sites affect nuclear entry. *J. Biol. Chem.* **282,** 28759–28767
32. Martínez-Bono, B., Quilis, I., Zalve, E., and Igual, J. C. (2010) Yeast karyopherins Kap123 and Kap95 are related to the function of the cell integrity pathway. *FEMS Yeast Res.* **10,** 28–37
33. Nguyen, A. N., Ikner, A. D., Shiozaki, M., Warren, S. M., and Shiozaki, K. (2002) Cytoplasmic localization of Wis1 MAPKK by nuclear export signal is important for nuclear targeting of Spc1/Sty1 MAPK in fission yeast. *Mol. Biol. Cell* **13,** 2651–2663
34. Gaits, F., and Russell, P. (1999) Active nucleocytoplasmic shuttling required for function and regulation of stress-activated kinase Spc1/StyI in fission yeast. *Mol. Biol. Cell* **10,** 1395–1407
35. Matsuyama, A., Arai, R., Yashiroda, Y., Shirai, A., Kamata, A., Sekido, S., Kobayashi, Y., Hashimoto, A., Hamamoto, M., Hiraoka, Y., Horinouchi, S., and Yoshida, M. (2006) ORFeome cloning and global analysis of protein localization in the fission yeast *Schizosaccharomyces pombe*. *Nat. Biotechnol.* **24,** 841–847
36. Martín, H., Flández, M., Nombela, C., and Molina, M. (2005) Protein phosphatases in MAPK signaling. We keep learning from yeast. *Mol. Microbiol.* **58,** 6–16
37. Chen, D., Wilkinson, C. R., Watt, S., Penkett, C. J., Toone, W. M., Jones, N., and Bähler, J. (2008) Multiple pathways differentially regulate global oxidative stress responses in fission yeast. *Mol. Biol. Cell* **19,** 308–317
38. Papadopoulou, K., Ng, S. S., Ohkura, H., Geymonat, M., Sedgwick, S. G., and McInerny, C. J. (2008) Regulation of gene expression during M-G_1-phase in fission yeast through Plo1p and forkhead transcription factors. *J. Cell Sci.* **121,** 38–47
39. Papadopoulou, K., Chen, J. S., Mead, E., Feoktistova, A., Petit, C., Agarwal, M., Jamal, M., Malik, A., Spanos, A., Sedgwick, S. G., Karagiannis, J., Balasubramanian, M. K., Gould, K. L., and McInerny, C. J. (2010) Regulation of cell cycle-specific gene expression in fission yeast by the Cdc14p-like phosphatase Clp1p. *J. Cell Sci.* **123,** 4374–4381
40. Westfall, P. J., Patterson, J. C., Chen, R. E., and Thorner, J. (2008) Stress resistance and signal fidelity independent of nuclear MAPK function. *Proc. Natl. Acad. Sci. U.S.A.* **105,** 12212–12217